

Prepared for *J. Phys. Chem. A*

March 20, 2007

**Thermochemical Kinetics of Hydrogen-Atom Transfers
Between Methyl, Methane, Ethynyl, Ethyne, and Hydrogen**

*Jingjing Zheng, Yan Zhao, and Donald G. Truhlar**

Department of Chemistry and Supercomputing Institute,
University of Minnesota, 207 Pleasant Street S.E.
Minneapolis, MN 55455-0431 USA

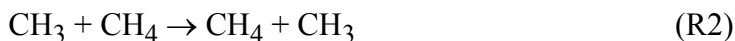
* Corresponding author: Donald G. Truhlar; e-mail: truhlar@umn.edu

Abstract

Saddle point properties of three symmetric and one asymmetric hydrogen–transfer and the energy of reaction of the asymmetric reactions are investigated in the present work. These reactions were calculated by various density functionals, many of which were developed in recent years, by coupled cluster theory, and by multicoefficient correlation methods based on wave function theory. Instead of comparing calculated results to “semi-experimental” values, we compared them to very accurate theoretical values (e.g., to values obtained by the Weizmann-1 method). Coupled cluster theory and the multicoefficient correlation methods MC–QCISD/3 and MCQCISD–MPW are very accurate for these reactions with mean unsigned errors below 0.94 kcal/mol. Diagnostics for multireference character add additional reliability to these results. The newly developed hybrid density functional M06-2X shows very good performance for these reactions with a mean unsigned error of only 0.77 kcal/mol; The BHandHLYP, MPW1K and BB1K density functionals, can also predict these reactions well with mean unsigned errors less than 1.42 kcal/mol.

1. Introduction

Recently, Temelso et al.¹ studied symmetric and asymmetric hydrogen transfer reactions by coupled cluster theory with quasiperturbative triple excitations² (CCSD(T)), Møller-Plesset second-order perturbation³ (MP2) theory, and two density functionals, B3LYP⁴⁻⁶ and BHLYP⁷. They attempted to judge the theoretical results by comparison to experimental activation energies. Their studies were especially complete for the reactions



for which they located high-level saddle points without imaginary frequencies. Their paper stimulates the present investigation in several respects: (i) For reaction R1, they did not compare to the essentially converged results of Mielke et al.⁸ We will make this comparison. (ii) For reaction R2, they did not compare to the multilevel results of Dybala-Defratyka et al.⁹ (iii) In the density functional calculations, they use only the cc-pVDZ¹⁰ and cc-pVTZ¹⁰ basis sets, which we will abbreviate as ccDZ and ccTZ. These basis sets do not include diffuse functions, although these are now known to be very important for density functional theory.¹¹ (iv) They compared to results obtained with old density functionals^{6,7} but not with modern ones. (v) Their comparisons with experiment were based on comparing harmonic conventional transition state theory¹² with Wigner transmission coefficients¹³ to Arrhenius fits over the temperature range 150–350 K, but the Wigner transmission coefficient is invalid for most cases where tunneling is significant and especially for the cases considered here. The Wigner formula is

$$\kappa = 1 + y \quad (1)$$

where y is defined as $(1/24)(\hbar\omega^\ddagger/k_B T)^2$, \hbar is Planck's constant divided by 2π , ω^\ddagger is the magnitude of the imaginary frequency at the saddle point, k_B is Boltzmann's constant, and T is temperature. Equation 1 represents the first two terms in an expansion in \hbar .

Clearly it is invalid if $y \geq 0.5$. For reactions R1 and R2, Ref. 1 used eq. 1 with $y = 2$ and 3, respectively.

With the above reasons as motivation, in the present work we re-examined the saddle point properties of the three symmetrical hydrogen transfer reactions R1 – R3 with various density functionals and multilevel methods. Instead of comparing to experimental barrier heights derived by harmonic conventional transition state theory, we adopted very accurate theoretical results (e. g. barrier heights calculated by the Weizmann–1 (W1)¹⁴⁻¹⁶ method) as the benchmarks, attempting to take advantage of state-of-art electronic structure theory's ability to often predict thermochemistry within ± 1 kcal/mol¹⁴ accuracy.

Due to the importance of the C₂H radical in interstellar space,¹⁷⁻²¹ planetary atmospheres,²² and high-temperature hydrocarbon combustion,^{23,24} we also studied the simplest asymmetric hydrogen-transfer reaction R4 involving C₂H radical, namely



2. Methods

In the present work, the barrier heights and energies of reaction of the investigated hydrogen–transfer reactions were calculated by various density functionals, most of which were developed in recent years (including many developed in the last four years), by coupled cluster theory with different treatments of triple excitation (CCSD(T)², LR–CCSD(T),^{25–27} and CCSDT^{28,29}), and by some multilevel methods based on wave function theory (WFT).

The density functional theory (DFT) methods include local DFT (BLYP,^{4,5} M06–L,³⁰ and VSXC³¹) and hybrid DFT. The latter may be subdivided into hybrid GGAs (B1LYP,³² B3LYP, B97-1,³³ B97-2,³³ B97-3,³⁴ B98,³⁵ BHandHLYP,^{4,7,36} MPW1K,^{37,38} mPW1PW,³⁷ O3LYP,^{4,39,40} and PBE0^{41,42}) and hybrid meta GGAs (B1B95,^{36,43} BB1K,⁴⁴ BMK,⁴⁵ M05,⁴⁶ M05–2X,⁴⁶ M06,⁴⁷ M06-2X,⁴⁷ M06-HF,⁴⁸ MPW1B95,⁴⁹ MPW1KCIS,^{43,50–53} MPWB1K,⁴⁹ MPWKCIS1K,^{43,50–53} PBE1KCIS,^{41,51–54} PW6B95,⁵⁵ PWB6K,⁵⁵ TPSS1KCIS,^{51–53,56–58} TPSSh,^{56,57} and τ HCTHh⁵⁹). Some of these functionals have more than one name in the literature. For example, the PBE0^{41,60} functional is also sometimes called PBE1PBE^{42,61} and PBEh^{62,63}. Note that in our notation, following Becke^{64,65} and others,^{66–68} “local” functionals denote functionals that depend on the magnitude of the local gradient of the spin densities and on the local spin kinetic energies, whereas “hybrid” functionals include a finite percentage of nonlocal exchange computed from the Kohn-Sham orbitals as in Hartree-Fock theory.

The multilevel wave function methods used here, in addition to W1, include CCSD(T), LR–CCSD(T), and CCSDT calculations at geometries optimized at some other

levels, and also the following multicoefficient correlation⁶⁹ methods: BMC-CCSD⁷⁰, G3SX(MP3)⁷¹, MCG3/3⁷², MC-QCISD/3⁷² and MCQCISD-MPW⁵⁸.

In most of the coupled cluster calculations employed here, the energy is calculated with the a basis set we denotes SccTZ ("semidiffuse" ccTZ), which denotes a basis set combination of accTZ (abbreviation of aug-cc-pVTZ^{10,73} where "aug" denotes diffuse basis functions) for heavy atoms and ccTZ for hydrogen atoms.

Except for the W1, G3SX(MP3), and coupled cluster calculations, all the geometries were optimized at the same theory level and with the same basis set as was used for the energy. We especially note that all BMC-CCSD, MCG3/3, MC-QCISD/3, and MCQCISD-MPW calculations were optimized at the multilevel.⁷⁴ The geometries used for the G3SX(MP3) method were optimized at B3LYP/6-31G(2df,p) level, because that is how the method is defined.⁷¹ W1 calculations were carried out at several different geometries. First we used the B97-1 density functional and the accTZ basis set. We choose this level because B97-1 is the recommended density functional for geometry optimization of large molecules as an alternative of the original proposed CCSD(T)/ccQZ method in the W2¹⁴ protocol; see Ref. 15 for more information. Furthermore, the aug-cc-pV(T+d)Z⁷⁵ is recommended by Martin¹⁶ for geometry optimization in the W1 and W2 theories. In our cases, aug-cc-pV(T+d)Z is identical to accTZ since only hydrogen and carbon atoms are involved. In addition to the B97-1/accTZ geometry, we also calculated W1 energies at geometries obtained with the MPW1K, BB1K and M06-2X density functionals and the MG3S¹¹ basis set to evaluate the effect of geometry choice on the W1 energies. For H and C atoms, MG3S is identical to 6-311+G(2df,2p)⁷⁶ basis set. Finally, we carried out W1 calculations at BMC-CCSD, MC-QCISD/3 and MCQCISD-

MPW geometries because these multilevel methods are accurate for both thermochemistry⁵⁸ and barrier heights,^{58,77} and are affordable enough to optimize transition state geometries.

In all coupled cluster calculations core electrons are uncorrelated (i.e., doubly occupied in all configurations, sometimes called frozen) when not indicated otherwise. We use “full” to indicate the case that all electrons are correlated in the calculations, e.g., CCSDT(full).

For reaction R1, we will use the converged barrier height of Mielke et al⁸ as our standard of comparison to test other methods, since their results are converged within ± 0.010 kcal/mol. For reaction R2 – R4, we consider the W1//BMC–CCSD results to be the most accurate available values because of the excellent performance shown by both W1¹⁴⁻¹⁶ and BMC–CCSD^{58,77} in previous assessments. These results will give improved estimates of the barrier heights and also serve to test more approximate methods.

All density functional calculations (except for the B97–1/accTZ and B3LYP/6-31G(2df,p) calculations mentioned above) were carried out with the MG3S¹¹ basis set, which is a very good choice for DFT methods based on its performance and cost.^{58,77}

We consider only unrestricted calculations in this paper except that for the single-level coupled cluster calculations, we used a spin–restricted calculation to obtain the orbitals, but a spin–unrestricted correlated calculation.

All single-level calculations in this work were performed using the *Gaussian03*⁷⁸ package except that B97-3, M05, M05-2X, M06, M06-2X, M06-HF, M06-L, PW6B95, and PWK6B were carried out with a locally modified version (MN-GFM⁷⁹) of *Gaussian03*. All multicoefficient correlation methods were carried out with the

*MLGAUSS*⁸⁰ program in conjunction with *Gaussian03*. The *MOLPRO* 2002.6 package⁸¹ was used for W1 calculations and CCSD(T) calculations that are not components of multi-coefficient correlation methods and. The *NWChem* 5.0 program⁸² was used for CCSD(T)(full), LR-CCSD(T)(full), and CCSDT(full) calculations.

3. Results and Discussions

In tables, R_{XH}^\ddagger is an X–H bond distance at the saddle point, and V^\ddagger is the classical barrier height.

3.1 Reaction $\text{H} + \text{H}_2 \rightarrow \text{H}_2 + \text{H}$

Table 1 compares the ccDZ and ccTZ calculations of Temelso et al.¹ as well as various DFT methods and multilevel methods to the best estimates of Mielke et al.⁸ for reaction R1. We also present some W1 calculations at several different geometries in Table 1 although the converged values are available. These barrier heights at the W1 level are very close to the converged value with discrepancies of less than 0.1 kcal/mol. Table 1 shows that coupled cluster theory with the ccDZ basis set overestimates the bond distances at the saddle point by 0.013 Å and overestimates the saddle point height by 0.2–0.4 kcal/mol. The density functional calculations included in the tables of Ref. 1 gave very inaccurate barrier heights of 3.0–6.5 kcal/mol for this reaction. However, some modern density functionals shown in Table 1 of the present article perform much better. Among all the methods in Table 1 except W1, the BMK functional gives the best prediction both for geometry, which is essentially the same as the converged value, and barrier height, with an overestimate of 0.14 kcal/mol. It is well known that local DFT methods and the popular B3LYP method usually underestimate barrier heights, but Table 1 shows that a few hybrid DFT methods overestimate the barrier heights of reaction R1; these functionals, with the amount of overestimate in kcal/mol in parentheses, are BMK (0.14), B97–2 (0.42), M05 (1.60), M05–2X (3.07), and M06–HF (6.56). All multilevel methods in Table 1 overestimate the barrier height but are within 0.75 kcal/mol of the accurate result. The multicoefficient correlation methods are more accurate than CCSD(T)/ccDZ for the saddle point geometry.

3.2 Reaction $\text{CH}_3 + \text{CH}_4 \rightarrow \text{CH}_4 + \text{CH}_3$

It is not clear if one should accept the results for reaction R1 as providing general guidance since R1 has only three electrons. We turn next to the 19-electron case in Table 2, where the five W1 calculations based on different geometries in Table 2 give very similar results, the difference being only 0.02 kcal/mol, although the saddle point geometries R_{CH}^\ddagger have differences up to 0.011 Å. These W1 calculations predict a barrier height of 17.82 – 17.84 kcal/mol. This is only 0.29 – 0.31 kcal/mol higher than the “consensus” value of Dybala-Defratyka et al.⁹, which is an average over the results of four multicoefficient correlation methods and one density functional method optimized for kinetics. Thus the CCSD(T)/ccTZ calculation of Ref. 1 is probably accurate within ~0.1 kcal/mol, whereas the comparison to experiment in Ref. 1 indicated it was too high by ~2.7 kcal/mol. The key point here is that high-level theoretical predictions can be more reliable than “semi-experimental” results, and they are recommended as standards when no accurate experimental result is available.

Among the methods tested for reaction R2, the G3SX calculation at the MP2(full)/6-31G geometry gives barrier heights almost the same as the W1 value, differing by only 0.01 kcal/mol. All DFT methods except BHandHLYP underestimate the barrier height of this reaction. M05 has the best performance for this barrier height among all the tested functionals; it underestimates the barrier height by only 0.36 kcal/mol. The saddle point geometries R_{CH}^\ddagger vary in the very narrow range of 1.330 – 1.348 Å for all the tested methods except VSXC and BLYP, which yield 1.350 Å and 1.356 Å, respectively.

3.3 Reactions Containing Ethynyl

Next we turn attention to reactions R3 and R4, which are harder cases because systems with multiple bonds have more near-degeneracy correlation effects than reactions like R2. The ethynyl radical is a particularly difficult case, with severe spin contamination and multireference character, as discussed next.

3.3.1 Spin Contamination

All the reactions studied in the present work contain open-shell species. Computations using unrestricted orbitals for open-shell system have the potential problem that the many-electron wave function can be significantly contaminated by higher-multiplicity spin states since the wave function in the unrestricted calculations is not necessarily an eigenfunction of the total spin. In most cases, spin contamination raises the energy since a higher-energy state is being mixed in. This affects calculations of the barrier height and reaction energy. If there is no spin contamination, the expectation value of the total spin, $\langle \hat{S}^2 \rangle$, should be equal to $S(S + 1)$ where S equals 1/2 times the number of unpaired electrons. For a doublet state the accurate expectation value $\langle \hat{S}^2 \rangle$ is 0.75.

Table 3 lists the $\langle \hat{S}^2 \rangle$ values of the studied radicals and transition states at the HF, MP2, DFT, CCSD, and QCISD levels. These methods are the components of some of the multicoefficient correlation methods used in the present study. As is well documented,⁸³⁻⁸⁵ CCSD(T) is relatively insensitive to spin contamination at the accuracy level of interest here, and Temelso et al.¹ showed that there is little spin contamination for all the species in reaction R1 – R4 at the UHF-UCCSD(T) level. In the present work, we always use ROHF orbitals as a reference for unrestricted CCSD(T), that is, the calculation is restricted to be a spin eigenfunction at the Hartree-Fock level but not at the post-Hartree-Fock level. Table 3 shows that the $\langle \hat{S}^2 \rangle$ values of CH₃ and the transition states of H + H₂ and CH₃ + CH₄ are between 0.76 and 0.79, which is not severe. But calculations at the HF, MP2, CCSD, and QCISD levels have serious spin contamination for C₂H and the transition states of C₂H + H₂ and C₂H + C₂H₂. This indicates that calculations by the multicoefficient correlation methods are also affected by spin contamination. Spin contamination is considered to be a minimal problem in density functional theory.⁸⁶ The two density functionals shown in Table 3 give $\langle \hat{S}^2 \rangle$ values

from 0.76 – 0.80 for all the species. Actually none of the density functionals used in this paper has large spin contamination.

3.3.2 Diagnostics of Multireference Character

To gain insight into the reliability of the W1 method for reactions containing the C₂H radical, we used six diagnostics for determining whether this system has significant multireference character, i.e., has significant nondynamical correlation energy. One approach is the T_1 ⁸⁷ diagnostic. A system should be considered to have multireference character when the T_1 diagnostic value exceeds 0.02.⁸⁷ We calculated the T_1 diagnostics with MOLPRO package, and we give T_1 diagnostic values of the saddle points of reaction R4 at different geometries in Table 4. The T_1 diagnostics of reactant and product are 0.015 – 0.016 for C₂H, 0.013 for C₂H₂, and 0.006 for H₂ at all the optimized geometries, and they are not shown in this table. It seems that the saddle point has some multireference character at the MC-QCISD/3 and M06-2X geometries, but there is also some uncertainty regarding the recommended T_1 diagnostic value for open-shell systems, and the T_1 diagnostic may not be a reliable indicator of multireference character for these systems.⁸⁸

Therefore we also consider the second diagnostic, which is to compare the results of CCSD(T) calculations based on using two different sets of reference orbitals. The supposition of this diagnostic is that single-reference systems will be insensitive to the choice of reference orbitals whereas multireference systems will be sensitive to the choice of reference orbitals. This approach was proposed by Beran et al.⁸⁹ and utilized by Villaume et al.⁹⁰ and Schultz et al.⁹¹ For this purpose, we calculated the forward barrier height and reaction energy of reaction R4 at the CCSD(T)/SccTZ level first using the orbitals obtained from a Hartree-Fock calculation (these are the standard orbitals for coupled cluster calculations) and second using orbitals obtained from a DFT calculation (using the BLYP functional). Two sets of barrier heights and reaction energies at different geometries are shown in Table 4. The differences are only ~0.1 kcal/mol for

barrier heights and ~ 0.5 kcal/mol for reaction energies. We see that the forward barrier height of this system is not overly sensitive to the choice of reference orbitals, and we conclude that W1 calculations of forward barrier height of reaction R4 are reliable. Nevertheless it is interesting to consider more diagnostics to get experience in whether the various diagnostics are reliable indicators of multireference character.

One sometimes expects that local functionals will be preferred for multireference systems because of their important near-degeneracy correlation effects.^{92,93} The third multireference diagnostic used here is B_I diagnostic,⁹⁴ which is based on this expectation. The B_I diagnostic is defined by the difference of the bond energies computed by BLYP and B1LYP//BLYP. Therefore, it refers to a bond breaking process. The recommended value of the B_I diagnostic is 10.0 (the B_I diagnostic value is divided by 1 kcal/mol to produce a unitless diagnostic). This means that a bond dissociation process should be considered to require multireference methods if the diagnostic exceeds 10. The computed B_I diagnostic value for C–H bond breaking of C_2H_2 is 0.4 with MG3S basis set; it is much smaller than the recommended 10.0. The B_I diagnostic and the diagnostic based on different reference orbitals give the same conclusion, namely that the C_2H radical is not dominated by multireference character.

The fourth multireference diagnostic is the one proposed by Martin and Parthiban⁹⁵ and by Sullivan et al.⁹⁶ They proposed that one should calculate the percentage of the most accurate estimate of the total atomization energy (TAE) that is accounted for by a single-configuration SCF calculation; significant multireference character is indicated if this value is below $\sim 50\%$. In the case of C_2H_2 we find a value of this diagnostic, indicated as %TAE(SCF), of $\sim 92\%$ (see Table 4). The values of C_2H and the transition state of the $H_2 + C_2H$ reaction are $\sim 65\%$ and $\sim 82\%$; they are all larger than 50% and show again that these systems are dominated by dynamical correlation, not by near-degeneracy correlation.

The fifth multireference diagnostic we used is the percentage of the CCSD(T) TAE that is accounted for by the (T) terms; this is indicated as %TAE[(T)].⁹⁷ In general, a value of %TAE[(T)] below 2% indicates system dominated by dynamical correlation; whereas %TAE[(T)] between 2% and about 4% – 5% indicates mild nondynamical correlation.⁹⁷ As shown in Table 4, the values of %TAE[(T)] of the saddle points of Reaction 4 at various geometries exceed 2% (2.4% – 2.6%). The values of %TAE[(T)] for C₂H₂ and C₂H are about 2.3% and 3.1%, respectively. The threshold value 2% is questionable, but this diagnostic at least indicates this reaction does not have severe or even moderate multireference character.

Sixth, as the final multireference diagnostic, we also compared the absolute energies of CCSDT, CCSD(T), and six variants of LR–CCSD(T) with cc-pVDZ(6D10F) and cc-pVTZ(6D10F) basis sets. All electrons were correlated, and ROHF orbitals were used in the calculations. The standard single, double, and quasiperturbative triples coupled cluster method, CCSD(T), has been shown to be well suited for describing single–reference system, but it is inadequate for system with large nondynamic correlation effects. The coupled cluster method with single, double, and triple excitations, CCSDT, can improve the results in such cases dramatically. The recently developed completely renormalized (CR)^{98,99} and locally renormalized (LR)²⁵⁻²⁷ CCSD(T) methods eliminate at least some of the failures of the standard CCSD(T) for accounting large nondynamic correlation effects. Furthermore, LR–CCSD(T) is size extensive if the orbitals are localized on noninteracting fragments. Table 5 shows the absolute energy deviations of CCSD(T) and LR–CCSD(T) relative to CCSDT energies. Here we consider that the CCSDT energies are the most accurate among these coupled cluster methods, although some authors might dispute this, since CCSD(T) is sometimes more accurate than CCSDT.^{100,101} The deviations of CCSD(T) from CCSD are quite small, especially with a triple zeta basis set. In general, the minimum requirement for a basis set to be able to reliably identify trends in CCSD(T) versus CCSDT comparisons is triple zeta, and

smaller basis sets may predict misleading trends.¹⁰² Some variants of LR-CCSD(T) give much larger errors than CCSD(T) methods. For a given method, the deviations from CCSDT are very similar for reactant, products, and transition state. This provide further evidence that it is reasonable to use W1 results as our best estimates for reaction R3 and R4.

3.3.3 Reaction $\text{HCC} + \text{HCCH} \rightarrow \text{HCCH} + \text{CCH}$

As a result of the above considerations, we consider W1//BMC-CCSD to be the best estimate and five other W1 calculations based on B97-1/accTZ, BB1K/MG3S, MC-QCISD/3, MCQCISD-MPW, and MPW1K/MG3S geometries were also performed for reaction R3 in order to test methods that are affordable for large systems.

Among DFT methods, BHandHLYP gives the closest barrier height to the W1 results; it overestimates the W1 results by only 0.49 kcal/mol; it is even better than CCSD(T)/ccTZ calculations at some geometries. The saddle point geometry and barrier height of our MPW1K/MG3S calculation are also very similar to those calculated at the MPW1K/6-311++G(3df,2p)//6-311++(d,p) level given by Nguyen *et al.*¹⁰³ The local DFT functional M06-L predicts this barrier height quite well with only a 1.20 kcal/mol underestimate, which is even better than some multilevel methods, such as BMC-CCSD, G3SX(MP3), MC-QCISD/3, MCQCISD-MPW, and CCSD(T)/ccTZ//ccDZ. All DFT methods except the BHandHLYP and M06-2X functionals underestimate the barrier height for this reaction. The barrier height of the CCSD(T)/ccTZ//ccDZ method which was taken as the standard result in Ref. 1, is lower than W1's result by ~1.3 kcal/mol. Again the fluctuation of the saddle point geometry is small. In particular, it is 1.268 to 1.280 Å for all methods except VSXC and BLYP, which yield 1.282 and 1.287 Å, respectively.

One surprising result is that the BMC-CCSD method gives a quite large error of 3.24 kcal/mol, although the magnitude of the deviation is only 0.24 and 0.28 kcal/mol for reactions R1 and R2, whereas MC-QCISD/3 still gives small error for this reaction.

BMC–CCSD has also been found to be the most accurate N^6 methods for DBH24 database.⁷⁷ One feature of BMC–CCSD is that it uses the MG3^{104,105} basis set which has diffuse functions on H as well as heavy atoms, however MC–QCISD/3 uses MG3S. Moran et al.¹⁰⁶ concluded that it is dangerous to use diffuse functions on hydrogen atoms with the 6-311G basis set when one uses correlated WFT for systems with double bonds. But Table 6 shows that CCSD(T) method with MG3 and MG3S basis sets give identical results and MP2/MG3 and MP2/MG3S calculations in Table 7 also give almost the same results. We conclude that employing diffuse functions on hydrogen atoms can be excluded as the source of the unexpectedly large error. The other feature of BMC–CCSD is that it uses a scheme that scales the MP4(DQ) energy increment separately instead of scaling the QCISD energy increment relative to MP2 directly as in the MC–QCISD/3 method. Furthermore the scaling coefficient c_4 for the CCSD energy increment relative to MP4(DQ) in BMC–CCSD is quite large, 1.55622; the scaling coefficient c_4 for the QCISD energy increment relative to MP2 in MC–QCISD/3 is only 1.1673. We list the barrier heights and reaction energies calculated by the components of BMC–CCSD and MC–QCISD/3 in Table 7. We found that MP2 and MP4(DQ) with small basis sets give quite large errors for the barrier height of reaction R3 and the reaction energy of reaction R4. The large coefficient c_4 of BMC–CCSD amplifies these large errors. These large errors are apparently caused by spin contaminations in the two reactions. The small error of forward barrier height of reaction R4 is due to the cancellation of spin contamination between the transition state and C₂H radical.

3.3.4 Reaction $\text{HCC} + \text{H}_2 \rightarrow \text{HCCH} + \text{H}$

In addition to the above three symmetric hydrogen–transfer reactions, we also studied the asymmetric hydrogen–transfer reaction R4. Table 8 compares forward and backward barrier heights and the reaction energies of multilevel methods and density functional calculations to the W1//BMC–CCSD values. The reason that we chose the BMC–CCSD geometry for the reference W1 calculations at the transition state is that it has the smallest CCSD(T)/SccTZ gradient among the six tested geometries shown in

Table 9. The W1 values of reaction energy at the various geometries are still very close, but the W1 barriers heights of this reaction are strongly dependent on geometry, although the barrier heights at the BMC–CCSD, MC–QCISD/3, MCQCISD–MPW, and M06–2X geometries, which are probably the most reliable ones in this case, are very close with only a spread of only 0.05 kcal/mol.

In Table 8, we assess the methods for reaction R4 by the deviations of the predicted reaction energy from that calculated by W1//BMC–CCSD. Except for the other W1 and coupled cluster calculations, the recently developed local density functional M06-L gives the best reaction energy; it only overestimates this reaction energy by 0.06 kcal/mol. The reaction energies calculated at the CCSDT and LR–CCSD(T) levels are consistent with the W1//BMC–CCSD results, which also confirms that W1 calculation is suitable for this system.

For reaction R4, WFT methods predict a very wide range of 1.810 – 1.722 Å for the saddle point distance R_{CH}^{\ddagger} of the forming C–H bond; for example, R_{CH}^{\ddagger} is 1.810 Å for MCQCISD–MPW, 1.770 Å for BMC-CCSD, 1.759 Å for MCG3/3, 1.749 Å for MC-QCISD/3, 1.723¹⁰⁷ Å for CCSD(T)/6-311++G(2df,2p), and 1.722¹ Å for CCSD(T)/ccDZ. In contrast, DFT methods predict this distance to be greater than 1.87 Å except that M06-2X gives 1.675 Å. For reactions whose forward barrier height is listed as a positive value in Table 8, there is a saddle point with only one imaginary frequency. For reactions whose forward barrier height is given as 0.00, the minimum energy path appears to be monotonically downhill from reactants to products or to a product van der Waals well; in such cases, the reactant potential is the highest–energy point on the minimum energy path. The table shows that most density functionals predict downhill minimum energy paths for this low barrier reaction. Only M06-2X, O3LYP, and MPW1K give forward barriers greater than 1.1 kcal/mol. The forward barrier height predicted by the recent M06-2X functional has only a 0.13 kcal/mol discrepancy compared to the W1//BMC–CCSD value. A few other functionals predict finite barriers below 1.0 kcal/mol, in particular BHandHLYP (0.95), MPWK CIS1K (0.83), BB1K (0.73), B1B95 (0.47), BMK (0.45), MPWB1K (0.30) and TPSS1KCIS (0.21).

The LR–CCSD(T) method, in three of its six variants, has an MUE for barrier heights and reaction energy of 0.16 kcal/mol or less. Feller et al.¹⁰² concluded that

CCSDT calculations only slightly improve CCSD(T) atomization energies when the wave function is dominated by the Hartree–Fock configuration. Thus the very small difference between CCSDT(full) and CCSD(T)(full) shown in Table 8 give another indication that the wave functions of this reaction are dominated by a single reference state. Considering the results in Table 6 and in Table 8 together, we find that the CCSD(T), MC–QCISD/3, and MCQCISD–MPW methods can treat reaction systems containing ethynyl radical very well both for barrier heights and for reaction energy.

3.4 All Four Reactions

In Table 10, we give the mean unsigned errors (MUE) of the five barrier heights and one nonzero reaction energy of the four reactions we have been discussing. The data set HCBH5 consists of the present data set of 5 hydrocarbon barrier heights, where hydrogen is considered as a special case of a hydrocarbon for convenience in naming the data set. The data set HCK6 is HCBH5 plus ΔE for reaction R4, where “K” stands for kinetics. We first discuss the last column of this table, which is an average over all six tests. The table shows that the CCSD(T), MC–QCISD/3 and MCQCISD–MPW methods have the lowest MUEs, which are in the range of 0.47 – 0.94 kcal/mol, except for the CCSD(T)/SccTZ//B97–1/accTZ method because B97–1/accTZ predicts that reaction R4 has a downhill energy profile. Based on the MUEs of the density functionals in Table 10, we conclude that the newly developed hybrid density functional M06-2X is the best hybrid density functional to describe these reactions; it has an MUE of only 0.77 kcal/mol, which is much better than the popular B3LYP functional (2.55 kcal/mol), and BHandHLYP, MPW1K, and BB1K also show good performance (1.27 – 1.42 kcal/mol). Considering its affordability for very large systems, the local density functional M06-L also shows good accuracy with a 1.81 kcal/mol MUE for barrier heights and reaction energy.

4. Concluding Remarks

In this work we give new best estimates of the barriers of hydrocarbon reactions R2–R4; these are obtained at the W1//BMC–CCSD level. Although a careful analysis of the expected reliability of the calculations was carried out, and all tests indicated that the methods should be reliable, one must still be cautious in light of the potential

multireference character of systems with π bonding. Nevertheless the calculations are more complete than the previously available ones, and they provide new best estimates of the barrier heights.

The new estimates of accurate barrier heights, along with the accurate barrier height of the $\text{H} + \text{H}_2$ reaction, are called the HCBH5 data set and were used to test a variety of high-level and affordable methods, in particular multilevel WFT methods, multicoefficient methods, and density functionals. In general, coupled cluster theory and the MC-QCISD/3 and MCQCISD-MPW multicoefficient correlation method are very accurate for these reactions with mean unsigned errors below 0.94 kcal/mol. Some modern density functionals, such as M06-2X, MPW1K BB1K and older BH and HLYP, and BB1K, are much more accurate than the popular and historically important B3LYP functional. The very recent M06-2X density functional shows especially good performance for these reactions with an MUE of only 0.77 kcal/mol. Considering its affordability for very large systems, the performance of M06-L is also noteworthy.

In Table 11, we list mean unsigned errors of methods tested against the DBH24 database⁷⁷ and the HCBH5 data set. The diverse and representative DBH24 database consists of four reaction types, in particular heavy-atom transfer, nucleophilic substitution, unimolecular and association, and hydrogen transfer reactions, and the component databases containing these kinds of barriers are called HATBH6, NSBH6, UABH6, and HTBH6, respectively. The HCBH5 data set contains hydrogen-atom transfers between hydrocarbons.

BMC-CCSD is the most accurate N^6 method for the DBH24 database, but it is less accurate for HCBH5 data set because of the spin contamination of the systems containing ethynyl and the large scaling coefficient c_4 in BMC-CCSD. G3SX(MP3) is also very accurate for DBH24 database but has a greater MUE for HCBH5; one reason is that the B3LYP/6-31G(2df,p) method predicts a downhill reaction path for reaction R4. Thus the new reactions studied here present difficult challenges for some methods that

have previously been very successful. However the multicoefficient correlation methods, MC-QCISD/3 and MCQCISD-MPW, and the hybrid density functionals, M06-2X, BB1K, and PWB6K are shown here to perform very well both for DBH24 database⁷⁷ and HCBH5 data set.

The HCBH5 and HCK6 data sets can be very useful to test new methods for thermochemical kinetics of hydrogen-atom transfer between hydrocarbons. In addition the new estimates of accurate barrier heights, presented here can be very useful for combustion modeling.

Acknowledgments. The authors are grateful to Mark Iron for helpful assistance. This work was supported in part by the U. S. Department of Energy, Office of Basic Energy Sciences, under grant No. DE-FG02-86ER13579 and was performed in part using the Molecular Science Computing Facility (MSCF) in the William R. Wiley Environmental Molecular Sciences Laboratory, a national scientific user facility sponsored by the U.S. Department of Energy's Office of Biological and Environmental Research and located at the Pacific Northwest National Laboratory, operated for the Department of Energy by Battelle.

References

- (1) Temelso, B.; Sherrill, C. D.; Merkle, R. C.; Freitas Jr, R. A. *J. Phys. Chem. A* **2006**, *110*, 11160.
- (2) Raghavachari, K.; Trucks, G. W.; Pople, J. A.; Head-Gordon, M. *Chem. Phys. Lett.* **1989**, *157*, 479.
- (3) Møller, C.; Plesset, M. S. *Phys. Rev.* **1934**, *46*, 618.
- (4) Lee, C.; Yang, W.; Parr, R. G. *Phys. Rev. B* **1988**, *37*, 785.
- (5) Becke, A. D. *J. Chem. Phys.* **1993**, *98*, 5648.
- (6) Kohn, W.; Becke, A. D.; Parr, R. G. *J. Phys. Chem.* **1996**, *100*, 12974.
- (7) Becke, A. D. *J. Chem. Phys.* **1993**, *98*, 1372.
- (8) Mielke, S. L.; Garrett, B. C.; Peterson, K. A. *J. Chem. Phys.* **2002**, *116*, 4142.
- (9) Dybala-Defratyka, A.; Paneth, P.; Pu, J.; Truhlar, D. G. *J. Phys. Chem. A* **2004**, *108*, 2475.
- (10) Dunning, T. H. *J. Chem. Phys.* **1989**, *90*, 1007.
- (11) Lynch, B. J.; Zhao, Y.; Truhlar, D. G. *J. Phys. Chem. A* **2003**, *107*, 1384.
- (12) Eyring, H. *J. Chem. Phys.* **1935**, *3*, 107.
- (13) Wigner, E. Z. *Phys. Chem. B* **1932**, *19*, 203.
- (14) Martin, J. M. L.; de Oliveira, G. *J. Chem. Phys.* **1999**, *111*, 1843.
- (15) Oren, M.; Iron, M. A.; Burcat, A.; Martin, J. M. L. *J. Phys. Chem. A* **2004**, *108*, 7752.
- (16) Martin, J. M. L. *J. Mol. Struct. (Theochem)* **2006**, *771*, 19.
- (17) Tucker, K. D.; Kutner, M. L.; Thaddeus, P. *Astrophys. J.* **1974**, *193*, L115.
- (18) Strobel, D. F. *Planetary and Space Science* **1982**, *30*, 839.
- (19) Jackson, W. M.; Bao, Y. H.; Urdahl, R. S. *Journal of Geophysical Research-Planets* **1991**, *96*, 17569.
- (20) Hasegawa, T. I.; Kwok, S. *Astrophysical Journal* **2001**, *562*, 824.
- (21) Markwick, A. J.; Ilgner, M.; Millar, T. J.; Henning, T. *Astronomy & Astrophysics* **2002**, *385*, 632.
- (22) Allen, M.; L., Y. Y.; Gladstone, G. R. *Icarus* **1992**, *100*, 527.
- (23) Shaub, W. M.; Bauer, S. H. *Combustion and Flame* **1978**, *32*, 35.
- (24) Boullart, W.; Devriendt, K.; Borms, R.; Peeters, J. *J. Phys. Chem.* **1996**, *100*, 998.
- (25) Kowalski, K. *J. Chem. Phys.* **2005**, *123*, 014102.
- (26) Wloch, M.; Gour, J. R.; Kowalski, K.; Picuch, P. *J. Chem. Phys.* **2005**, *122*, 214107.
- (27) Kowalski, K.; Picuch, P. *J. Chem. Phys.* **2005**, *122*, 074107.
- (28) Noga, J.; Bartlett, R. J. *J. Chem. Phys.* **1987**, *86*, 7041.
- (29) Scuseria, G. E.; Schaefer III, H. F. *Chem. Phys. Lett.* **1988**, *152*, 382.
- (30) Zhao, Y.; Truhlar, D. G. *J. Chem. Phys.* **2006**, *125*, 194101.
- (31) Van Voorhis, T.; Scuseria, G. E. *J. Chem. Phys.* **1998**, *109*, 400.
- (32) Adamo, C.; Barone, V. *Chem. Phys. Lett.* **1997**, *274*, 242.
- (33) Hamprecht, F. A.; Cohen, A. J.; Tozer, D. J.; Handy, N. C. *J. Chem. Phys.* **1998**, *109*, 6264.
- (34) Keal, T. W.; Tozer, D. J. *J. Chem. Phys.* **2005**, *123*.
- (35) Schmider, H. L.; Becke, A. D. *J. Chem. Phys.* **1998**, *108*, 9624.

- (36) Becke, A. D. *Phys. Rev. A* **1988**, *38*, 3098.
- (37) Adamo, C.; Barone, V. *J. Chem. Phys.* **1998**, *108*, 664.
- (38) Lynch, B. J.; Fast, P. L.; Harris, M.; Truhlar, D. G. *J. Phys. Chem. A* **2000**, *104*, 4811.
- (39) Hoe, W. M.; Cohen, A. J.; Handy, N. C. *Chem. Phys. Lett.* **2001**, *341*, 319.
- (40) Handy, N. C.; Cohen, A. J. *Mol. Phys.* **2001**, *99*, 403.
- (41) Adamo, C.; Barone, V. *J. Chem. Phys.* **1999**, *110*, 6158.
- (42) Ernzerhof, M.; Scuseria, G. E. *J. Chem. Phys.* **1999**, *110*, 5029.
- (43) Becke, A. D. *J. Chem. Phys.* **1996**, *104*, 1040.
- (44) Zhao, Y.; Lynch, B. J.; Truhlar, D. G. *J. Phys. Chem. A* **2004**, *108*, 2715.
- (45) Boese, A. D.; Martin, J. M. L. *J. Chem. Phys.* **2004**, *121*, 3405.
- (46) Zhao, Y.; Schultz, N. E.; Truhlar, D. G. *J. Chem. Phys.* **2005**, *123*.
- (47) Zhao, Y.; Truhlar, D. G. *Theor. Chem. Acc. (Mark Gordon 65th Birthday Issue)*, submitted.
- (48) Zhao, Y.; Truhlar, D. G. *J. Phys. Chem. A* **2006**, *110*, 13126.
- (49) Zhao, Y.; Truhlar, D. G. *J. Phys. Chem. A* **2004**, *108*, 6908.
- (50) Rey, J.; Savin, A. *Int. J. Quantum Chem.* **1998**, *69*, 581.
- (51) Krieger, J. B.; Chen, J.; Iafrate, G. J.; Savin, A. *Electron Correlations and Materials Properties*; Gonis, A., Kioussis, N., Eds.; Plenum: New York, 1999; pp 463.
- (52) Toulouse, J.; Savin, A.; Adamo, C. *J. Chem. Phys.* **2002**, *117*, 10465.
- (53) Zhao, Y.; Gonzalez-Garcia, N.; Truhlar, D. G. *J. Phys. Chem. A* **2005**, *109*, 2012.
- (54) Zhao, Y.; Truhlar, D. G. *J. Chem. Theory Comput.* **2005**, *1*, 415.
- (55) Zhao, Y.; Truhlar, D. G. *J. Phys. Chem. A* **2005**, *109*, 5656.
- (56) Staroverov, V. N.; Scuseria, G. E.; Tao, J. M.; Perdew, J. P. *J. Chem. Phys.* **2003**, *119*, 12129.
- (57) Tao, J. M.; Perdew, J. P.; Staroverov, V. N.; Scuseria, G. E. *Phys. Rev. Lett.* **2003**, *91*.
- (58) Zhao, Y.; Lynch, B. J.; Truhlar, D. G. *Phys. Chem. Chem. Phys.* **2005**, *7*, 43.
- (59) Boese, A. D.; Handy, N. C. *J. Chem. Phys.* **2002**, *116*, 9559.
- (60) Vydrov, O. A.; Scuseria, G. E. *J. Chem. Phys.* **2006**, *125*, 234109.
- (61) Hay, P. J.; Martin, R. L.; Uddin, J.; Scuseria, G. E. *J. Chem. Phys.* **2006**, *125*, 34712.
- (62) Barone, V.; Peralta, J. E.; Scuseria, G. E. *Nano Letters* **2005**, *5*, 1830.
- (63) Vydrov, O. A.; Scuseria, G. E.; Perdew, J. P.; Ruzsinszky, A.; Csonka, G. *I. J. Chem. Phys.* **2006**, *124*.
- (64) Becke, A. D. *J. Chem. Phys.* **1992**, *96*, 2155.
- (65) Becke, A. D. *J. Chem. Phys.* **1998**, *109*, 2092.
- (66) Van Leeuwen, R.; Baerends, E. J. *Phys. Rev. A* **1994**, *49*, 2421.
- (67) Dalcorso, A.; Resta, R. *Phys. Rev. B* **1994**, *50*, 4327.
- (68) Arbuznikov, A. V.; Kaupp, M. *Chem. Phys. Lett.* **2003**, *381*, 495.
- (69) Fast, P. L.; Corchado, J. C.; Sanchez, M. L.; Truhlar, D. G. *J. Phys. Chem. A* **1999**, *103*, 5129.
- (70) Lynch, B. J.; Zhao, Y.; Truhlar, D. G. *J. Phys. Chem. A* **2005**, *109*, 1643.

- (71) Curtiss, L. A.; Redfern, P. C.; Raghavachari, K.; Pople, J. A. *J. Chem. Phys.* **2001**, *114*, 108.
- (72) Lynch, B. J.; Truhlar, D. G. *J. Phys. Chem. A* **2003**, *107*, 3898.
- (73) Kendall, R. A.; Dunning, T. H.; Harrison, R. J. *J. Chem. Phys.* **1992**, *96*, 6796.
- (74) Rodgers, J. M.; Fast, P. L.; Truhlar, D. G. *J. Chem. Phys.* **2000**, *112*, 3141.
- (75) Dunning, T. H.; Peterson, K. A.; Wilson, A. K. *J. Chem. Phys.* **2001**, *114*, 9244.
- (76) Hehre, W. J.; Radom, L.; Schleyer, P. v. R.; Pople, J. A. *Ab Initio Molecular Orbital Theory*; Wiley: New York, 1986.
- (77) Zheng, J.; Zhao, Y.; Truhlar, D. G. *J. Chem. Theory Comput.* **2007**, *3*, 569.
- (78) Frisch, M. J.; Trucks, G. W.; Schlegel, H. B.; Scuseria, G. E.; Robb, M. A.; Cheeseman, J. R.; Zakrzewski, V. G.; Montgomery, J. A.; Stratmann, R. E.; Burant, J. C.; Dapprich, S.; Millam, J. M.; Daniels, A. D.; Kudin, K. N.; Strain, M. C.; Farkas, O.; Tomasi, J.; Barone, V.; Cossi, M.; Cammi, R.; Mennucci, B.; Pomelli, C.; Adamo, C.; Clifford, S.; Ochterski, J.; Petersson, G. A.; Ayala, P. Y.; Cui, Q.; Morokuma, K.; Malick, D. K.; Rabuck, A. D.; Raghavachari, K.; Foresman, J. B.; Cioslowski, J.; Ortiz, J. V.; Baboul, A. G.; Stefanov, B. B.; Liu, G.; Liashenko, A.; Piskorz, P.; Komaromi, I.; Gomperts, R.; Martin, R. L.; Fox, D. J.; Keith, T.; Al-Laham, M. A.; Peng, C. Y.; Nanayakkara, A.; Challacombe, M.; Gill, P. M. W.; Johnson, B. G.; Chen, W.; Wong, M. W.; Andres, J. L.; Gonzalez, C.; Head-Gordon, M.; Replogle, E. S.; Pople, J. A. Gaussian03; Revision D.01. Gaussian, Inc.: Pittsburgh, PA, 2003.
- (79) Zhao, Y.; Truhlar, D. G. MN-GFM: Minnesota Gaussian Functional Module; version 2.0.1. University of Minnesota: Minneapolis, 2006.
- (80) Zhao, Y.; Truhlar, D. G. MLGAUSS; Version 2.0. University of Minnesota: Minneapolis, 2006.
- (81) Werner, H.-J.; Knowles, P. J.; Amos, R. D.; Bernhardsson, A.; Berning, A.; Celani, P.; Cooper, D. L.; Deegan, M. J. O.; Dobbyn, A. J.; Eckert, F.; Hampel, C.; Hetzer, G.; Korona, T.; Lindh, R.; Lloyd, A. W.; McNicholas, S. J.; Manby, F. R.; Meyer, W.; Mura, M. E.; Nicklass, A.; Palmieri, P.; Pitzer, R.; Rauhut, G.; Scht|z, M.; Schumann, U.; Stoll, H.; Stone, A. J.; Tarroni, R.; Thorsteinsson, T. MOLPRO; 2002.6. University of Birmingham: Birmingham, 2002.
- (82) Bylaska, E. J.; Jong, W. A. d.; Kowalski, K.; Straatsma, T. P.; Valiev, M.; Wang, D.; Aprà, E.; Windus, T. L.; Hirata, S.; Hackler, M. T.; Zhao, Y.; Fan, P.-D.; Harrison, R. J.; Dupuis, M.; Smith, D. M. A.; Nieplocha, J.; Tipparaju, V.; Krishnan, M.; Auer, A. A.; Nooijen, M.; Brown, E.; Cisneros, G.; Fann, G. I.; Früchtl, H.; Garza, J.; Hirao, K.; Kendall, R.; Nichols, J. A.; Tsemekhman, K.; Wolinski, K.; Anchell, J.; Bernholdt, D.; Borowski, P.; Clark, T.; Clerc, D.; Dachsel, H.; Deegan, M.; Dyll, K.; Elwood, D.; Glendening, E.; Gutowski, M.; Hess, A.; Jaffe, J.; Johnson, B.; Ju, J.; Kobayashi, R.; Kutteh, R.; Lin, Z.; Littlefield, R.; Long, X.; Meng, B.; Nakajima, T.; Niu, S.; Pollack, L.; Rosing, M.; Sandrone, G.; Stave, M.; Taylor, H.; Thomas, G.; Lenthe, J. v.; Wong, A.; Zhang, Z. NWChem, A Computational Chemistry Package for Parallel Computers; 5.0. Pacific Northwest National Laboratory; Richland, Washington 99352-0999, USA, 2006.
- (83) Stanton, J. F. *J. Chem. Phys.* **1994**, *101*, 371.
- (84) Krylov, A. I. *J. Chem. Phys.* **2000**, *113*, 6052.

- (85) Szalay, P. G.; Vazquez, J.; Simmons, C.; Stanton, J. F. *J. Chem. Phys.* **2004**, *121*, 7624.
- (86) Baker, J.; Scheiner, A.; Andzelm, J. *Chem. Phys. Lett.* **1993**, *216*, 380.
- (87) Lee, T. J.; Taylor, P. R. *Int. J. Quantum Chem. Symp.* **1989**, *23*, 199.
- (88) Lambert, N.; Kaltsoyannis, N.; Price, S. D.; Zabka, J.; Herman, Z. *J. Phys. Chem. A* **2006**, *110*, 2898.
- (89) Beran, G. J. O.; Gwaltney, S. R.; Head-Gordon, M. *Phys. Chem. Chem. Phys.* **2003**, *5*, 2488.
- (90) Villaume, S.; Daniel, C.; Strich, A.; Perera, S. A.; Bartlett, R. J. *J. Chem. Phys.* **2005**, *122*, 44313.
- (91) Schultz, N. E.; Gherman, B. F.; Cramer, C. J.; Truhlar, D. G. *J. Phys. Chem. B* **2006**, *110*, 24030.
- (92) Perdew, J. P.; Emzerhof, M.; Burke, K. *J. Chem. Phys.* **1996**, *105*, 9982.
- (93) Schultz, N. E.; Zhao, Y.; Truhlar, D. G. *J. Phys. Chem. A* **2005**, *109*, 4388.
- (94) Schultz, N. E.; Zhao, Y.; Truhlar, D. G. *J. Phys. Chem. A* **2005**, *109*, 11127.
- (95) Martin, J. M. L.; Parthiban, S. In *Quantum-Mechanical Prediction of Thermochemical Data*; Cioslowski, J., Ed.; Kluwer Academic: Dordrecht, 2001; pp 31.
- (96) Sullivan, M. B.; Iron, M. A.; Redfern, P. C.; Martin, J. M. L.; Curtiss, L. A.; Radom, L. *J. Phys. Chem. A* **2003**, *107*, 5617.
- (97) Karton, A.; Rabinovich, E.; Martin, J. M. L.; Ruscic, B. *J. Chem. Phys.* **2006**, *125*, 144108.
- (98) Kowalski, K.; Piecuch, P. *J. Chem. Phys.* **2000**, *113*, 18.
- (99) Piecuch, P.; Kowalski, K. In *Computational Chemistry: Reviews of Current Trends*; Leszczynski, J., Ed.; World Scientific: Singapore, 2000; Vol. 5; pp 1.
- (100) Stanton, J. F. *Chem. Phys. Lett.* **1997**, *281*, 130.
- (101) Bomble, Y. J.; Stanton, J. F.; Kallay, M.; Gauss, J. *J. Chem. Phys.* **2005**, *123*, 54101.
- (102) Feller, D.; Dixon, D. A. *J. Chem. Phys.* **2001**, *115*, 3484.
- (103) Nguyen, H. M. T.; Chandra, A. K.; Carl, S. A.; Nguyen, M. T. *J. Mol. Struct. (Theochem)* **2005**, *732*, 219.
- (104) Fast, P. L.; Sanchez, M. L.; Truhlar, D. G. *Chem. Phys. Lett.* **1999**, *306*, 407.
- (105) Curtiss, L. A.; Redfern, P. C.; Raghavachari, K.; Rassolov, V.; Pople, J. A. *J. Chem. Phys.* **1999**, *110*, 4703.
- (106) Moran, D.; Simmonett, A. C.; III, F. E. L.; Allen, W. D.; Schleyer, P. v. R.; III, H. F. S. *J. Am. Chem. Soc.* **2006**, *128*, 9342.
- (107) Peeters, J.; Ceursters, B.; Nguyen, H. M. T.; Nguyen, M. T. *J. Chem. Phys.* **2002**, *116*, 3700.

Table 1. Saddle Point Properties for Reaction $\text{H} + \text{H}_2 \rightarrow \text{H}_2 + \text{H}$ (Energy in kcal/mol and Distance in Å) *a,b*

Method	Ref.	R_{HH}^\ddagger	V^\ddagger	ΔV^\ddagger
Local DFT				
M06-L	present	0.925	6.42	-3.19
VSXC	present	0.928	5.55	-4.06
BLYP	present	0.935	2.96	-6.65
Hybrid GGA DFT				
B97-2	present	0.928	10.03	0.42
B97-1	present	0.929	9.05	-0.56
B97-3	present	0.928	8.94	-0.67
B98	present	0.929	8.04	-1.57
MPW1K	present	0.924	7.19	-2.42
BHandHLYP	present	0.924	6.54	-3.07
mPW1PW	present	0.928	5.96	-3.65
PBE0	present	0.930	5.76	-3.85
B1LYP	present	0.929	4.86	-4.75
B3LYP	present	0.930	4.32	-5.29
O3LYP	present	0.928	4.05	-5.56
Hybrid meta GGA DFT				
BMK	present	0.930	9.75	0.14
τ HCTHh	present	0.931	8.98	-0.63
PWB6K	present	0.924	8.92	-0.69
BB1K	present	0.926	8.56	-1.05
M06	present	0.927	8.51	-1.10

Table 1. Continued

Method	Ref.	R_{HH}^{\ddagger}	V^{\ddagger}	ΔV^{\ddagger}
MPWB1K	present	0.926	8.47	-1.14
M05	present	0.930	11.21	1.60
M06-2X	present	0.930	11.66	2.05
B1B95	present	0.929	7.56	-2.05
MPW1B95	present	0.929	7.51	-2.10
PW6B95	present	0.926	7.39	-2.22
M05-2X	present	0.930	12.68	3.07
MPWKCIS1K	present	0.924	5.94	-3.67
TPSS1KCIS	present	0.926	5.60	-4.01
PBE1KCIS	present	0.930	4.31	-5.30
MPW1KCIS	present	0.930	3.98	-5.63
M06-HF	present	0.935	16.17	6.56
TPSSh	present	0.932	0.74	-8.87
Single-level WFT				
Converged	8	0.930	9.61	0.00
CCSD(T)/ccDZ	1	0.943	10.0	0.4
Multi-level WFT				
W1//MCQCISD–MPW	present	0.932	9.66	0.05
W1//BMC–CCSD	present	0.932	9.67	0.06
W1//MC–QCISD/3	present	0.931	9.67	0.06
W1//B97–1/accTZ	present	0.929	9.67	0.06
W1//BB1K	present	0.926	9.68	0.07
W1//MPW1K	present	0.924	9.68	0.07

Table 1. Continued

Method	Ref.	R_{HH}^{\ddagger}	V^{\ddagger}	ΔV^{\ddagger}
CCSD(T)/ccTZ//ccDZ	1	0.943	9.8	0.2
BMC-CCSD	present	0.932	9.85	0.24
CCSD(T)/SaccTZ//MCQCISD-MPW	present	0.932	10.00	0.39
CCSD(T)/SaccTZ//MC-QCISD/3	present	0.931	10.01	0.40
CCSD(T)/SaccTZ//BB1K	present	0.926	10.01	0.40
CCSD(T)/SaccTZ//B97-1/accTZ	present	0.929	10.01	0.40
CCSD(T)/SaccTZ//MPW1K	present	0.924	10.02	0.41
MCQCISD-MPW ^c	present	0.932	8.99	-0.62
G3SX(MP3)	present	0.932	10.35	0.74
MC-QCISD/3	present	0.931	10.36	0.75
MCG3/3	present	0.938	10.36	0.75
CCSD(T)/MG3//M06-2X	present	0.930	10.46	0.85
CCSD(T)MG3S//M06-2X	present	0.930	10.48	0.87

^aIn tables, the basis set for DFT calculations is MG3S when not indicated otherwise.

^bIn each section of the tables, the methods are listed in order of increasing magnitude of the deviation from the converged values. The last column of the table is the signed deviation from the converged value.

^c This method is listed in the multilevel WFT section since we can consider it to be a multilevel WFT calculation with a DFT component. It can also be considered to be a fifth-rung DFT, just as hybrid and hybrid meta DFT methods, which contain Hartree-Fock exchange, can be considered to be fourth-rung DFT methods.

Table 2. Saddle Point Properties for Reaction $\text{CH}_3 + \text{CH}_4 \rightarrow \text{CH}_4 + \text{CH}_3$ (Energy in kcal/mol and Distance in Å) *a,b*

Method	Ref.	R_{CH}^\ddagger	V^\ddagger	ΔV^\ddagger
Local DFT				
M06-L	present	1.342	15.48	-2.34
VSXC	present	1.350	15.18	-2.46
BLYP	present	1.356	13.55	-4.27
Hybrid GGA DFT				
MPW1K	present	1.333	17.31	-0.51
B1LYP	present	1.346	16.87	-0.95
BHandHLYP	present	1.337	19.65	1.83
O3LYP	present	1.341	15.98	-1.84
B3LYP	present	1.346	15.71	-2.11
B97-3	present	1.341	15.67	-2.15
mPW1PW	present	1.339	15.12	-2.70
B97-2	present	1.340	14.30	-3.52
PBE0	present	1.338	14.20	-3.62
PBE1KCIS	present	1.338	13.61	-4.21
B98	present	1.344	13.59	-4.22
B97-1	present	1.343	12.98	-4.84
Hybrid meta GGA DFT				
M05	present	1.346	17.46	-0.36
BB1K	present	1.333	17.00	-0.82
BMK	present	1.341	16.98	-0.84
MPWKCIS1K	present	1.332	16.83	-0.99

Table 2. Continued

Method	Ref.	R_{CH}^\ddagger	V^\ddagger	ΔV^\ddagger
M05-2X	present	1.340	16.79	-1.03
PWB6K	present	1.330	16.76	-1.06
M06-2X	present	1.338	16.76	-1.06
M06	present	1.346	16.75	-1.07
MPWB1K	present	1.331	16.52	-1.30
M06-HF	present	1.338	16.31	-1.51
B1B95	present	1.338	15.39	-2.43
PW6B95	present	1.337	15.10	-2.72
TPSS1KCIS	present	1.345	14.91	-2.91
MPW1B95	present	1.335	14.89	-2.93
TPSSh	present	1.353	13.46	-4.36
MPW1KCIS	present	1.341	13.38	-4.44
τ HCTHh	present	1.345	12.46	-5.36
Multilevel WFT				
W1//BMC-CCSD	present	1.339	17.82	0.00
W1//B97-1/accTZ	present	1.344	17.82	0.00
W1//MC-QCISD/3	present	1.338	17.81	-0.01
W1//MCQCISD-MPW	present	1.340	17.81	-0.01
G3SX//MP2(full)/6-31G(d)	9	1.331	17.81	-0.01
W1//MPW1K	present	1.333	17.84	0.02
W1//BB1K	present	1.333	17.84	0.02
CCSD(T)/ccTZ//ccDZ	1	1.344	17.8	0.0
G3SX(MP3)//B3LYP/6-31G(2df,p)	9	1.348	17.74	-0.08

Table 2. Continued

Method	Ref.	R_{CH}^\ddagger	V^\ddagger	ΔV^\ddagger
MCG3/3	9	1.342	17.90	0.08
MCG3/3//MPW1K/6-31+G(d,p)	9	1.334	17.93	0.11
CCSD(T)/SccTZ//MPW1K	present	1.333	17.66	-0.16
CCSD(T)/SccTZ//BB1K	present	1.333	17.66	-0.16
MC-QCISD/3	present	1.339	17.98	0.16
CCSD(T)/SccTZ//MCQCISD-MPW	present	1.340	17.64	-0.18
CCSD(T)/SccTZ//MC-QCISD/3	present	1.338	17.64	-0.18
CCSD(T)/SccTZ//B97-1/accTZ	present	1.344	17.63	-0.19
BMC-CCSD	present	1.339	17.54	-0.28
Consensus	9	1.335	17.53	-0.29
MCQCISD-MPW ^c	present	1.340	17.27	-0.55
CCSD(T)/MG3//M06-2X	present	1.338	18.45	0.63
CCSD(T)/MG3S//M06-2X	present	1.338	18.48	0.66

^a In tables, the basis set for DFT calculations is MG3S when not indicated otherwise.

^b In each section of the tables, the methods are listed in order of increasing magnitude of the deviation from the converged values. The last column of the table is the signed deviation from the converged value.

^c This method is listed in the multilevel WFT section since we can consider it to be a multilevel WFT calculation with a DFT component. It can also be considered to be a fifth-rung DFT, just as hybrid and hybrid meta DFT methods, which contain Hartree-Fock exchange, can be considered to be fourth-rung DFT methods.

Table 3 Expectation values of Total Spin, $\langle \hat{S}^2 \rangle$, for Selected Species Using Different Methods ^a.

Species	HF	MP2	MPW1K	M06-L	CCSD	QCISD
CH ₃	0.76	0.76	0.76	0.76	0.76	0.75
CCH	1.12	1.02	0.80	0.78	1.17	1.17
H-H-H	0.79	0.79	0.76	0.76	0.79	0.79
CH ₃ -H-CH ₃	0.79	0.79	0.76	0.76	0.79	0.79
HCC-H-CCH	1.22	1.11	0.80	0.78	1.41	1.41
HCC-H-H	1.07	1.02	0.80	0.78	1.18	1.18

^a In this table, the basis set is MG3S. The geometries were optimized at the corresponding theory level except BMC-CCSD geometries were used for CCSD and QCISD calculations.

Table 4 T_I Diagnostics of Multireference Character and and %TAE[(T)] for the Saddle Point, Forward Barrier Height, and Reaction Energy of Reaction R4 Calculated at the CCSD(T)/SccTZ Level Based on Hartree–Fock and Kohn–Sham Orbitals, Respectively.^a

Geometry	T_I diagnostic	%TAE[(T)]	%TAE[(SCF)]	Forward BH		Reaction Energy	
				HF ^b	KS ^b	HF ^b	KS ^b
MCQCISD-MPW	0.019	2.5	82.0	2.09	1.98	-29.49	-30.02
MC-QCISD/3	0.021	2.6	81.7	2.16	2.05	-29.52	-30.05
BB1K/MG3S	0.016	2.4	83.0	1.35	1.27	-29.54	-30.06
MPW1K/MG3S	0.017	2.4	82.7	1.75	1.66	-29.53	-30.05
M06-2X/MG3S	0.021	2.5	81.6	2.21	2.11	-29.42	-29.95

^a KS orbitals are obtained from BLYP calculations.

^b HF means Hartree–Fock orbitals and KS means Kohn–Sham orbitals.

Table 5 A comparison of CCSD, CCSD(T), and LR-CCSD(T) energies with the corresponding CCSDT results at BMC-CCSD geometries. All electrons were correlated. The CCSDT results represent total energies in hartrees. The energies of other methods are given in millihartrees relative to CCSDT energy values.

Method	C ₂ H ₂	CCH	HCC-H-H
Basis set: ccDZ(6D10F)			
CCSDT(full)	-77.120571	-76.410770	-77.569477
CCSD(full)	12.009	12.204	13.050
CCSD(T)(full)	0.345	0.408	0.384
LR-CCSD(T)(full), IA	2.063	2.042	2.058
LR-CCSD(T)(full), IB	2.799	2.836	3.025
LR-CCSD(T)(full), IIA	1.212	1.138	1.072
LR-CCSD(T)(full), IIB	1.857	1.932	2.039
LR-CCSD(T)(full), IIIA	0.042	0.072	-0.095
LR-CCSD(T)(full), IIIB	0.824	0.969	0.998
Basis set: ccTZ(6D10F)			
CCSDT(full)	-77.225436	-76.504212	-77.673779
CCSD(full)	17.090	16.992	18.148
CCSD(T)(full)	0.040	0.081	0.038
LR-CCSD(T)(full), IA	2.209	2.170	2.171
LR-CCSD(T)(full), IB	3.106	3.051	3.247
LR-CCSD(T)(full), IIA	1.032	1.062	0.970
LR-CCSD(T)(full), IIB	1.929	1.944	2.046
LR-CCSD(T)(full), IIIA	-0.312	-0.236	-0.443
LR-CCSD(T)(full), IIIB	0.635	0.756	0.763

Table 6. Saddle Point Properties for Reaction $\text{HCC} + \text{HCCH} \rightarrow \text{HCCH} + \text{HCC}$ (Energy in kcal/mol and Distance in Å) *a,b*

Method	Ref.	R_{CH}^\ddagger	V^\ddagger	ΔV^\ddagger
Local DFT				
M06-L	present	1.280	11.58	-1.20
BLYP	present	1.287	6.56	-6.23
VSXC	present	1.282	2.29	-10.49
Hybrid GGA DFT				
BHandHLYP	present	1.269	13.28	0.49
MPW1K	present	1.268	12.09	-0.70
B1LYP	present	1.277	10.22	-2.57
O3LYP	present	1.277	10.03	-2.75
B97-3	present	1.275	9.84	-2.95
mPW1PW	present	1.273	9.61	-3.17
B3LYP	present	1.278	9.09	-3.70
PBE0	present	1.274	8.66	-3.13
B97-2	present	1.275	7.65	-5.13
B98	present	1.276	6.95	-5.84
B97-1	present	1.276	6.26	-6.53
Hybrid meta GGA DFT				
M06-2X	present	1.277	13.08	0.29
MPWK CIS1K	present	1.269	11.62	-1.17
M06	present	1.283	11.57	-1.22
BB1K	present	1.270	11.28	-1.51
PWB6K	present	1.268	10.94	-1.84

Table 6. Continued.

Method	Ref.	R_{CH}^{\ddagger}	V^{\ddagger}	ΔV^{\ddagger}
MPWB1K	present	1.269	10.82	-1.97
BMK	present	1.274	10.34	-2.45
M05-2X	present	1.274	10.15	-2.64
B1B95	present	1.275	9.45	-3.33
TPSS1KCIS	present	1.277	9.11	-3.68
MPW1B95	present	1.273	9.00	-3.79
PW6B95	present	1.273	8.91	-3.88
M05	present	1.283	8.57	-4.22
PBE1KCIS	present	1.275	7.98	-4.81
MPW1KCIS	present	1.277	7.75	-5.04
TPSSh	present	1.282	7.28	-5.51
M06-HF	present	1.270	5.58	-7.21
τ HCTHh	present	1.277	5.46	-7.33
Multilevel WFT				
W1//BMC-CCSD	present	1.276	12.79	0.00
CCSD(T)/MG3S//M06-2X	present	1.277	12.59	-0.20
CCSD(T)/MG3//M06-2X	present	1.277	12.55	-0.24
W1//MPW1K	present	1.268	12.49	-0.30
W1//BB1K/MG3S	present	1.270	12.47	-0.32
W1//MCQCISD-MPW	present	1.275	12.45	-0.33
W1//B97-1Z	present	1.276	12.44	0.35
W1//MC-QCISD/3	present	1.275	12.43	-0.35
CCSD(T)/SccTZ//MPW1K	present	1.268	12.03	-0.75

Table 6. Continued.

Method	Ref.	R_{CH}^\ddagger	V^\ddagger	ΔV^\ddagger
CCSD(T)/SccTZ//BB1K	present	1.270	12.01	-0.78
CCSD(T)/SccTZ//B97-1/accTZ	present	1.276	11.99	-0.80
CCSD(T)/SccTZ//MC-QCISD/3	present	1.275	11.94	-0.85
CCSD(T)/SccTZ//MCQCISD-MPW	present	1.275	11.85	-0.93
MC-QCISD/3	present	1.275	11.54	-1.25
CCSD(T)/ccTZ//ccDZ	1	1.281	11.5	-1.3
MCQCISD-MPW ^c	present	1.275	10.65	-2.14
G3SX(MP3)//B3LYP/6-31G(2df,p)	present	1.273	10.16	-2.63
BMC-CCSD	present	1.276	9.54	-3.24

^aIn tables, the basis set for DFT calculations is MG3S when not indicated otherwise.

^bIn each section of the tables, the methods are listed in order of increasing magnitude of the deviation from the converged values. The last column of the table is the signed deviation from the converged value.

^c This method is listed in the multilevel WFT section since we can consider it to be a multilevel WFT calculation with a DFT component. It can also be considered to be a fifth-rung DFT, just as hybrid and hybrid meta DFT methods, which contain Hartree–Fock exchange, can be considered to be fourth-rung DFT methods.

Table 7 A Comparison of Barrier Heights and Reaction Energies with Methods of BMC–CCSD and MC–QCISD/3 and Their Components for Reactions R1 – R4. All the calculations were based on BMC–CCSD geometries. (unit: kcal/mol)

	MP2/MG3	MP2/MG3S	HF/MG3	HF/MG3S	CCSD/6-31B(d)	QCISD/6-31G(d)	MP2/6-31B(d)	MP2/6-31G(d)	HF/6-31B(d)	HF/6-31G(d)	MP4(DQ)/6-31B(d)
V_1^\ddagger	13.80	13.82	17.62	17.62	15.43	14.91	17.68	17.17	18.73	17.83	16.69
V_2^\ddagger	19.69	19.72	31.06	31.06	22.22	22.25	21.96	22.23	30.61	30.37	23.28
V_3^\ddagger	24.10	24.13	27.21	27.23	17.95	17.31	27.25	27.30	27.04	26.41	25.87
V_{4f}^\ddagger	3.08	3.11	8.04	8.05	4.95	4.87	4.80	4.71	7.82	7.67	5.43
ΔE_4	-49.49	-49.51	-24.28	-24.29	-31.43	-30.67	-50.57	-50.39	-24.57	-23.87	-42.62

Table 8. Barrier Heights and Reaction Energies for Reaction $\text{HCC} + \text{H}_2 \rightarrow \text{HCCH} + \text{H}$ (Energy in kcal/mol and Distance in Å) ^a

Method	R_{CH}^\ddagger	$V_f^\ddagger b$	$V_r^\ddagger c$	ΔE	MUE ^d
Local DFT					
M06-L	---	0.00	30.31	-30.31	1.38
BLYP	---	0.00	29.34	-29.34	1.98
VSXC	---	0.00	39.20	-39.20	5.96
Hybrid GGA DFT					
BHandHLYP	1.875	0.95	31.82	-30.87	0.74
MPW1K/6-311++G(3df,2p)//6-311G++(d,p) ^e	1.916	1.1	30.4	-29.3	1.3
mPW1PW	---	0.00	32.21	-32.21	1.38
B3LYP	---	0.00	30.22	-30.22	1.40
MPW1K	1.928	1.16	33.51	-32.35	1.40
B1LYP	---	0.00	30.18	-30.18	1.42
PBE0	---	0.00	33.33	-33.33	2.05
B97-3	---	0.00	33.35	-33.35	2.06
B98	---	0.00	33.61	-33.61	2.24
O3LYP	2.020	1.21	28.59	-27.38	2.48
B97-2	---	0.00	34.51	-34.51	2.86
B97-1	---	0.00	35.39	-35.39	3.43
Hybrid meta GGA DFT					
M06-2X	1.675	1.94	31.71	-29.77	0.40
MPWKCIS1K	1.966	0.83	33.15	-32.33	1.38
B1B95	2.336	0.47	32.89	-32.42	1.45
M05	---	0.00	30.47	-30.47	1.38
MPW1KCIS	---	0.00	31.96	-31.96	1.38

Table 8 Continued

Method	R_{CH}^{\ddagger}	$V_f^{\ddagger b}$	$V_r^{\ddagger c}$	ΔE	MUE ^d
PW6B95	---	0.00	32.42	-32.42	1.44
BB1K	2.035	0.73	33.54	-32.81	1.70
PBE1KCIS	---	0.00	32.92	-32.92	1.78
MPW1B95	---	0.00	33.22	-33.22	1.98
TPSS1KCIS	2.134	0.21	29.73	-29.52	1.72
M06	---	0.00	29.50	-29.50	1.88
MPWB1K	2.072	0.30	33.74	-33.44	2.13
PWB6K	2.018	0.02	33.92	-33.90	2.43
τ HCTHh	---	0.00	33.94	-33.94	2.46
BMK	2.823	0.45	35.05	-34.60	2.90
M05-2X	---	0.00	35.22	-35.22	3.31
TPSSh	---	0.00	26.44	-26.44	3.92
M06-HF	---	0.00	38.96	-38.96	5.80
Multilevel WFT					
W1//BMC-CCSD	1.770	2.07	32.32	-30.25	0.00
W1//MCQCISD-MPW	1.810	2.03	32.16	-30.13	0.10
W1//MC-QCISD/3	1.749	2.08	32.16	-30.08	0.11
W1//M06-2X	1.675	2.04	32.12	-30.08	0.13
LR-CCSD(T)(full),IA/ccTZ(6D10F)//BMC-CCSD	1.770	1.81	32.27	-30.46	0.13
LR-CCSD(T)(full),IB/ccTZ(6D10F)//BMC-CCSD	1.770	1.93	32.38	-30.45	0.13
LR-CCSD(T)(full),IIB/ccTZ(6D10F)//BMC-CCSD	1.770	1.88	32.37	-30.49	0.16
CCSDT(full)/ccTZ(6D10F)//BMC-CCSD	1.770	1.81	32.30	-30.48	0.17
CCSD(T)(full)/ccTZ(6D10F)//BMC-CCSD	1.770	1.78	32.29	-30.51	0.19
LR-CCSD(T)(full),IIIB/ccTZ(6D10F)//BMC-CCSD	1.770	1.82	32.38	-30.56	0.21

Table 8 Continued

Method	R_{CH}^{\ddagger}	$V_f^{\ddagger b}$	$V_r^{\ddagger c}$	ΔE	MUE d
LR-CCSD(T)(full),IIA/ccTZ(6D10F)//BMC-CCSD	1.770	1.75	32.26	-30.50	0.21
LR-CCSD(T)(full),IIIA/ccTZ(6D10F)//BMC-CCSD	1.770	1.68	32.21	-30.53	0.26
W1//MPW1K	1.928	1.73	31.87	-30.14	0.30
CCSD(T)/MG3S//M06-2X	1.675	2.53	32.20	-29.67	0.38
CCSD(T)/MG3//M06-2X	1.675	2.49	32.14	-29.65	0.40
CCSD(full) /ccTZ(6D10F)//BMC-CCSD	1.770	2.54	32.96	-30.42	0.43
MC-QCISD/3	1.749	2.48	32.01	-29.53	0.48
CCSD(T)/SccTZ//MC-QCISD/3	1.749	2.16	31.69	-29.52	0.49
CCSD(T)/SccTZ//MCQCISD-MPW	1.810	2.09	31.58	-29.49	0.51
W1//BB1K	2.035	1.36	31.50	-30.14	0.54
CCSD(T)/SccTZ//M06-2X	1.675	2.21	31.64	-29.42	0.55
CCSD(T)/SccTZ//MPW1K	1.928	1.75	31.28	-29.53	0.69
MCQCISD-MPW g	1.810	1.79	31.16	-29.38	0.77
CCSD(T)/ccTZ//ccDZ f	1.722	2.0	33.5	-31.5	0.8
CCSD(T)/SccTZ//BB1K	2.035	1.35	30.98	-29.54	0.95
W1//B97-1/accTZ	---	0.00	30.12	-30.12	1.47
CCSD(T)/SccTZ//B97-1/accTZ	---	0.00	29.49	-29.49	1.89
MCG3/3	1.759	2.37	29.67	-27.31	1.96
BMC-CCSD	1.770	2.00	28.97	-26.97	2.23
G3SX(MP3)//B3LYP/6-31G(2df,p)	---	0.00	28.98	-28.98	2.23

a In tables, the basis set for DFT calculations is MG3S when not indicated otherwise. In this table all results are from the present work except where indicated otherwise.

^b For reactions where the forward barrier height is given as 0.00, the minimum energy path appear to be monotonically downhill from reactant to product or to a product van der Waals well.

^c The backward barrier height is obtained by forward barrier height minus reaction energy.

^d MUE is the mean unsigned error in V_f^\ddagger , V_r^\ddagger , and ΔE , as compared to W1//BMC-CCSD.

^e From Ref. 101.

^f From Ref. 1.

^g This method is listed in the multilevel WFT section since we can consider it to be a multilevel WFT calculation with a DFT component. It can also be considered to be a fifth-rung DFT, just as hybrid and hybrid meta DFT methods, which contain Hartree-Fock exchange, can be considered to be fourth-rung DFT methods.

Table 9 Internal–Coordinate Components of CCSD(T)/SccTZ Single–Point Gradients at the Six Saddle Point Geometries of Reaction R4 Optimized at a variety of Levels. ^a (in Hartree/Å)

Geometry	R _{C1H1}	R _{C1C2}	R _{C2H2}	R _{H2H3}
MCQCISD-MPW	-0.00008	-0.03242	-0.00254	0.00554
MC-QCISD/3	0.00110	-0.02562	0.00005	0.00233
BMC–CCSD	-0.00049	0.01218	-0.00121	0.00111
BB1K/MG3S	-0.00907	-0.08845	-0.00616	-0.00224
MPW1K/MG3S	-0.00364	-0.06320	-0.00602	0.00112
M06-2X/MG3S	-0.00181	-0.07233	0.00371	-0.00652

^a The atoms are labeled as H1 – C1 – C2 – H2 – H3 in linear structure.

Table 10 Mean Unsigned Errors (kcal/mol) in Five Barrier Heights and One Reaction

Energy. *a,b*

Method	HCBH5 <i>c</i>	HCK6 <i>d</i>
Local DFT		
M06-L	2.16	1.81
BLYP	4.44	3.85
VSXC	5.23	5.85
Hybrid GGA DFT		
BHandHLYP	1.40	1.27
MPW1K	1.15	1.30
B97-3	1.77	1.99
B1LYP	2.49	2.09
mPW1PW	2.34	2.28
B3LYP	3.05	2.55
O3LYP	2.95	2.93
B97-2	2.68	2.94
PBE0	2.94	2.96
B98	3.00	3.06
B97-1	3.41	3.70
Hybrid meta GGA DFT		
M06-2X	0.83	0.77
BB1K	1.19	1.42
M06	1.65	1.50
MPWKCIS1K	1.58	1.66
M05	2.02	1.72
MPWB1K	1.52	1.80
PWB6K	1.45	1.81
BMK	1.56	2.02

Table 10 Continued

Method	HCBH5 ^c	HCK6 ^d
B1B95	2.00	2.03
PW6B95	2.20	2.19
MPW1B95	2.36	2.46
TPSS1KCIS	3.01	2.63
M05-2X	2.34	2.78
MPW1KCIS	3.50	3.21
PBE1KCIS	3.40	3.28
τ HCTHh	3.29	3.32
TPSSh	5.34	5.08
M06-HF	4.80	5.45
	Multilevel WFT	
CCSD(T)/SccTZ//BMC-CCSD	0.41	0.47
CCSD(T)/SccTZ//MC-QCISD/3	0.43	0.48
CCSD(T)/MG3S//M06-2X	0.46	0.48
CCSD(T)/MG3//M06-2X	0.46	0.49
CCSD(T)/SccTZ//MCQCISD-MPW	0.45	0.51
CCSD(T)/SccTZ//MPW1K	0.53	0.57
MC-QCISD/3	0.58	0.60
CCSD(T)/SccTZ//BB1K	0.70	0.70
CCSD(T)/ccTZ//ccDZ ^e	0.6	0.7
MCQCISD-MPW ^f	0.95	0.94
CCSD(T)/SccTZ//B97-1/accTZ	1.10	1.05
G3SX(MP3)//B3LYP/6-31G(2df,p)	1.77	1.69
BMC-CCSD	1.44	1.74

^a In tables, the basis set for DFT calculations is MG3S when not indicated otherwise.

^b Errors are measured with respect to the most accurate available results in all cases. For R1 this is the converged result of Ref. 8, and for R2–R4 it is the W1//MCQCISD-MPW results of the present paper.

^c HCBH5 is the present data set of 5 hydrocarbon barrier heights, where hydrogen is considered as a special case of a hydrocarbon for convenience in naming the data set. The result tabulated is the average over the absolute values of the errors in the five barrier heights of reaction R1 – R4.

^d The results are listed in each section in order of increasing values of this column, which is the hydrocarbon kinetics data set consisting of the five values in HCBH5 plus ΔE for reaction R4.

^e From Ref. 1

^f This method is listed in the multilevel WFT section since we can consider it to be a multilevel WFT calculation with a DFT component. It can also be considered to be a fifth-rung DFT, just as hybrid and hybrid meta DFT methods, which contain Hartree–Fock exchange, can be considered to be fourth-rung DFT methods.

Table 11 Mean Unsigned Errors of Methods Tested Against HCBH5 and DBH24 Data Sets.^a

Method	HATBH6	NSBH6	UABH6	HTBH6	HCBH5	average ^b
Local DFT						
M06-L	7.22	3.25	2.58	4.32	2.16	3.91
VSXC	7.53	4.90	1.49	4.98	5.23	4.83
BLYP	13.01	8.64	3.19	7.83	4.44	7.42
Hybrid GGA DFT						
MPW1K	1.36	1.15	2.42	1.40	1.15	1.50
BHandHLYP	2.60	1.32	1.92	2.17	1.40	1.88
B97-3	2.93	1.07	1.63	2.29	1.77	1.94
B97-2	4.46	1.63	1.81	3.21	2.68	2.76
mPW1PW	5.73	2.00	1.93	3.95	2.34	3.19
B98	5.39	3.05	1.84	4.00	3.00	3.46
B97-1	5.45	3.21	1.68	4.14	3.41	3.58
PBE0	6.45	1.99	1.96	4.62	2.94	3.59
B3LYP	7.38	3.44	1.69	4.73	3.05	4.06
O3LYP	7.98	5.14	2.19	4.45	2.95	4.54
Hybrid meta GGA DFT						
M06-2X ^c	1.04	0.80	1.09	1.18	0.83	0.99
BB1K	1.09	1.17	1.57	1.14	1.19	1.23
PWB6K	1.05	0.96	1.59	1.22	1.45	1.25
MPWB1K	1.16	1.01	1.63	1.32	1.52	1.33
BMK	1.58	0.86	2.06	1.20	1.56	1.45
M05-2X	1.96	1.48	1.60	1.40	2.34	1.76
MPWKCIS1K	2.20	1.48	3.35	1.97	1.58	2.12
M06 ^c	4.30	1.67	1.91	1.77	1.65	2.26
B1B95	4.46	1.22	1.12	3.14	2.00	2.39
M05	5.09	1.00	2.48	1.64	2.02	2.45
MPW1B95	4.37	1.26	1.23	3.38	2.36	2.52
PW6B95	4.92	2.08	1.17	3.46	2.20	2.77

Table 11 Continued.

Method	HATBH6	NSBH6	UABH6	HTBH6	HCBH5	average ^b
M06-HF	4.11	1.74	1.69	1.95	4.80	2.86
PBE1KCIS	8.21	1.90	2.80	5.71	3.40	4.40
TPSS1KCIS	8.45	4.95	1.66	4.99	3.01	4.61
MPW1KCIS	9.45	4.44	2.61	6.36	3.50	5.27
TPSSh	10.75	5.82	2.94	6.72	5.34	6.31
Multilevel WFT						
MC-QCISD/3	1.22	0.46	0.61	0.91	0.58	0.76
BMC-CCSD	1.36	0.54	0.40	0.57	1.44	0.86
MCQCISD-MPW	1.46	0.70	0.99	0.50	0.95	0.92
G3SX(MP3) ^d	1.18	0.73	0.40	0.51	1.77	0.92

^a The basis set for DFT calculations is MG3S when not indicated otherwise. Data for DBH24 are taken from Ref. 77, except where indicated otherwise. The geometries in DBH24 were optimized at QCISD/MG3 level. In HCBH5, energy calculations and geometry optimizations were carried out at the same level except G3SX(MP3) in this table.

^b Average of previous five columns.

^c DBH24 data for these methods are from the present work.

^d Geometries were optimized at the B3LYP/6-31G(2df,p) level for HCBH5 data set and at the QCISD/MG3 level for DBH24 database.